



ISSN: 0975-833X

RESEARCH ARTICLE

DFT STUDY OF BENZANNULATED LUTIDINEBISSTANNYLENE –TIN(II) MONOXIDE MOLECULE

*Oriabi, D. T., Raheem, H. N., Hassan, S. A., Hussain, Z. M., Kadhem, L. H. and Bahjat R. J. Muhyedeen

Theoretical Research Lab, College of Education for Girls, University of Kufa, Iraq

ARTICLE INFO

Article History:

Received 08th May, 2015
Received in revised form
07th June, 2015
Accepted 23rd July, 2015
Published online 31st August, 2015

Key words:

Density Functional Theory Calculations,
computational chemistry, Benzannnnulated
Lutidine tin(II) complex , Theoretical IR
spectrum, Theoretical NMR spectrum .

ABSTRACT

Quantum density functional theory (DFT) calculations for benzannulatedlutidine bisstannylene-tin(II) monoxide molecule is carried out. To explore the proper functional for our molecule, we perform DFT calculations with different hybrid functional. The results show that B3LYP is the best among the others. We calculated the theoretical IR for benzannulatedbisstannylene-tin(II) monoxide Molecule using B3LYP/SDD with scaling factor 0.961 which confirms the lutidine moiety is perpendicular to Sn- group. The HOMO-LUMO energy gap is very low of 80.46 meV. The Sn NMR spectrum showed that Sn₃located at downfield in comparison to Sn₁ and Sn₂.

Copyright © 2015 Oriabi et al. This is an open access article distributed under the Creative Commons Attribution License, which permits unrestricted use, distribution, and reproduction in any medium, provided the original work is properly cited.

Citation: Oriabi, D. T., Raheem, H. N., Hassan, S. A., Hussain, Z. M., Kadhem, L. H. and Bahjat R. J. Muhyedeen, 2015. "DFT study of BENZ annulated lutidinebisstannylene-tin(II) monoxide molecule", *International Journal of Current Research*, 7, (8), 19757-19762.

INTRODUCTION

Over the last years, complexes of N-heterocyclic carbenes have attracted much interest in the fields of coordination chemistry and homogenous catalysis (Hopkinson *et al.*, 2014 and Hahn *et al.*, 2006) due to their ability to tune the steric bulk about the ligating carbon centers, their salts are stable without decomposition in air and the ease of synthesis (Martin *et al.*, 2011 and Braunschweig *et al.*, 2012). The chemistry of their heavier analogues, germylenes (Neumann, 1991), plumbylenes (Erickson *et al.*, 2015), silylenes (Hashimoto *et al.*, 2015) and stannylens, have also attracted considerable (Ochiai *et al.*, 2015) interest because they can act as σ/π -donors and π -acceptors due to the presence of a vacant p-orbital and an unshared electron pair at the Si, Ge or Sn atom. In contrast to carbenes, the stannylens exhibit singlet ground states with a formal $5s^25p^2$ valence electron configuration. Some studies demonstrated that benzannulated monostannylens Bu_2Sn Oplays a significant role as catalysis in polymerization (Alessandro *et al.*, 2009 and Bernard, 1992) and as anti cancer (Navakoski *et al.*, 2013). Some researchers support their experimental studies by theoretical studies to investigate the exact electronic structure and to find the

physical and chemical properties and the proposed mechanism. Sindlinger and Wesemann optimized their dimeric platinum–stannylene complexes by means of DFT computations using BP86/[def2svp(C,H,N)-def2QZVP+ECP(Pt,Sn)] starting from the preliminary X-ray structure with hydrides H_1 & H_2 intuitively added between the platinum atoms and Sn_2 . They supported their suggestion for the geometrical arrangement within the $[Pt_2H_2Sn_2]$ -core by NMR spectroscopic characteristics (Sindlinger and Wesemann, 2015). De Proft's group previously reported that they reproduced the experimental NMR chemical shifts of the stannylene $Sn\{N[Si(CH_3)_3]_2\}_2$ by DFT/NMR calculations, demonstrating the interaction strength with various solvent molecules were via σ - and π - coordinating power (De Proft *et al.*, 2013).

Müller *et al* used density functional theory DFT/MPW1K/SDD(Sn) and 6-31G(d) level of theory to support their proposed mechanism regarding the cyclic disilylated stannylene complexes (Arp *et al.*, 2011). In this article, we carried out a comparative study among DFT functional fixing the basis set SDD to investigate the best functional that give a closer values for bond lengths and bond angles for Benzannulated Lutidine Bisstannylene-Tin(II) Monoxide, BLBTM, molecule which prepared by Hahn and co-workers (Alexander *et al.*, 2008) (Figure 1).

*Corresponding author: Oriabi, D. T.,
Theoretical Research Lab, College of Education for Girls, University
of Kufa, Iraq

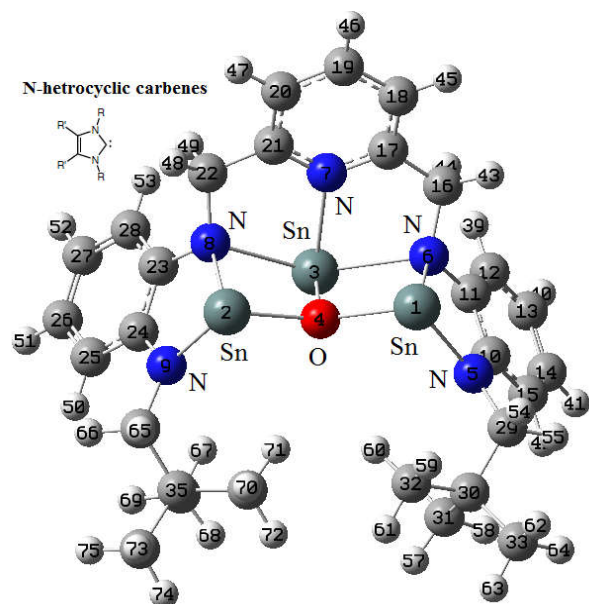


Figure 1. Molecular structure of BLBTM and coordination environment of the tin atoms

Computational details

The input geometry of BLBTM molecule derived from the X-ray coordinates. It was optimized by way of density functional theory (DFT) methods using seven various hybrid functionals. The tested DFT methods are: B3LYP/aut=all, B3PW91/aut=all, CAM-B3LYP, MPW1PW91, WB97XD, HSEH and PBE1PBE with QZV density fitting approximation in conjunction with the Stuttgart-Dresden- Dunning SDD effective core potential (ECP) basis set. These methods are summarized in Table 1. The DFT methods employed were also compared with the Hartree-Fock calculations. All the theoretical calculations were carried out in gas phase. Calculations were performed with the Gaussian 09 suite of programs.

RESULTS AND DISCUSSION

Geometry

Trying to find the best functional, we calculated the geometries for BLBTM molecule with DFT; B3LYP, B3PW91, CAM-B3LYP, MPW1PW91, WB97XD, HSEH and PBE1PBE levels of theory. The results were compared with experimental bond length and angle values reported for geometrical parameters of BLBTM. Figure 2 shows the correlations between the theoretical and the experimental values. Table 2 contains theoretical parameters of the optimized geometries; and as it can be observed, all tested methods showed good results for bond lengths, in particular when compared with the reported X-ray data. The B3LYP correlation is the best among the other while the HF method give less accurate correlation as seen in Figure 2. The optimized structure shows that the bond N₇-Sn₃-O₄ value is equal to 87.32° which means the Lutidine moiety is coordinated in perpendicular orientation relative to the Sn-O group. This value is very close to the X-ray value 93.75° of Hahn *et al.* (2006).

HOMO-LUMO, charge density and NMR spectrum

The quantum picture regarding the HOMO and LUMO of the molecular semiconductors that they are responsible for the reactivity of the molecule during the reaction and they give a significant indication about the selection of the reacted species. They also correspond to valence band maximum VBM and conduction band minimum CBM respectively in the inorganic semiconductors. Figure 3 shows that the HOMO 133 comes from bisstannylene moiety mainly while the LUMO 134 comes from lutidine moiety mainly. The two arbitrary colors (green and red) represent the positive and negative isosurface. HOMO/LUMO energy level difference, or energy gap, gives 85.46 meV (or 14507.86 nm) and between HOMO 133 and LUMO 139 is 0.16804 eV or (7378.26 nm).

Table 1. Summary of DFT methods tested in the study

No	Method	Type	Exchange/correlation functional
1	B3LYP	Hybrid DFT	Becke88/Lee-Yang-Parr
2	B3PW91	Hybrid DFT	non-local correlation Perdew/Wang
3	CAM-B3LYP	Hybrid DFT	Handy and coworkers' long range corrected version of B3LYP using the Coulomb-attenuating method
4	PBE1PBE	Hybrid DFT	This functional uses 25% exchange and 75% correlation weighting
5	WB97XD	Hybrid DFT	Head-Gordon/ uses a version of Grimme's D2 dispersion model
6	HSEH1PBE	Hybrid DFT	Heyd-Scuseria-Ernzerhof
7	MPW1PW91	Hybrid DFT	Modified Perdew-Wang

Table 2. The correlation of experimental and theoretical bond lengths and angles

Bonds	Methods							Exp.
	MPW1PW91	B3PW91	WB97XD	HSEH	CAM-B3LYP	B3LYP	PBE1PBE	
Sn ₂ -O ₄	2.162	2.168	2.149	2.163	2.152	2.171	2.19365	2.114
Sn ₂ -N ₉	2.113	2.118	2.101	2.115	2.104	2.131	2.13593	2.098
Sn ₂ -N ₈	2.264	2.269	2.271	2.268	2.259	2.275	2.28424	2.202
Sn ₁ -O ₄	2.150	2.157	2.140	2.150	2.140	2.158	2.18143	2.135
Sn ₁ -N ₆	2.261	2.266	2.235	2.267	2.256	2.272	2.28115	2.211
Sn ₁ -N ₅	2.123	2.128	2.131	2.126	2.116	2.130	2.14479	2.103
Sn ₃ -O ₄	2.108	2.112	2.103	2.111	2.098	2.108	2.13687	2.079
Sn ₃ -N ₇	2.389	2.393	2.387	2.392	2.386	2.400	2.40397	2.294
Sn ₃ -N ₈	2.431	2.440	2.387	2.439	2.430	2.461	2.47075	2.370
Sn ₃ -N ₆	2.472	2.479	2.554	2.480	2.476	2.498	2.50836	2.393
R ²	0.9861	0.9878	0.9418	0.9872	0.9869	0.9910	0.9901	
angles								
O ₄ -Sn ₃ -N ₇	88.00	88.10	89.08	88.00	87.40	87.32	87.95	93.75
N ₈ -Sn ₃ -N ₆	130.40	130.50	128.14	130.34	131.00	130.84	130.86	131.87
Sn ₂ -O ₄ -Sn ₁	127.81	127.55	134.38	128.04	129.01	128.49	127.57	124.70

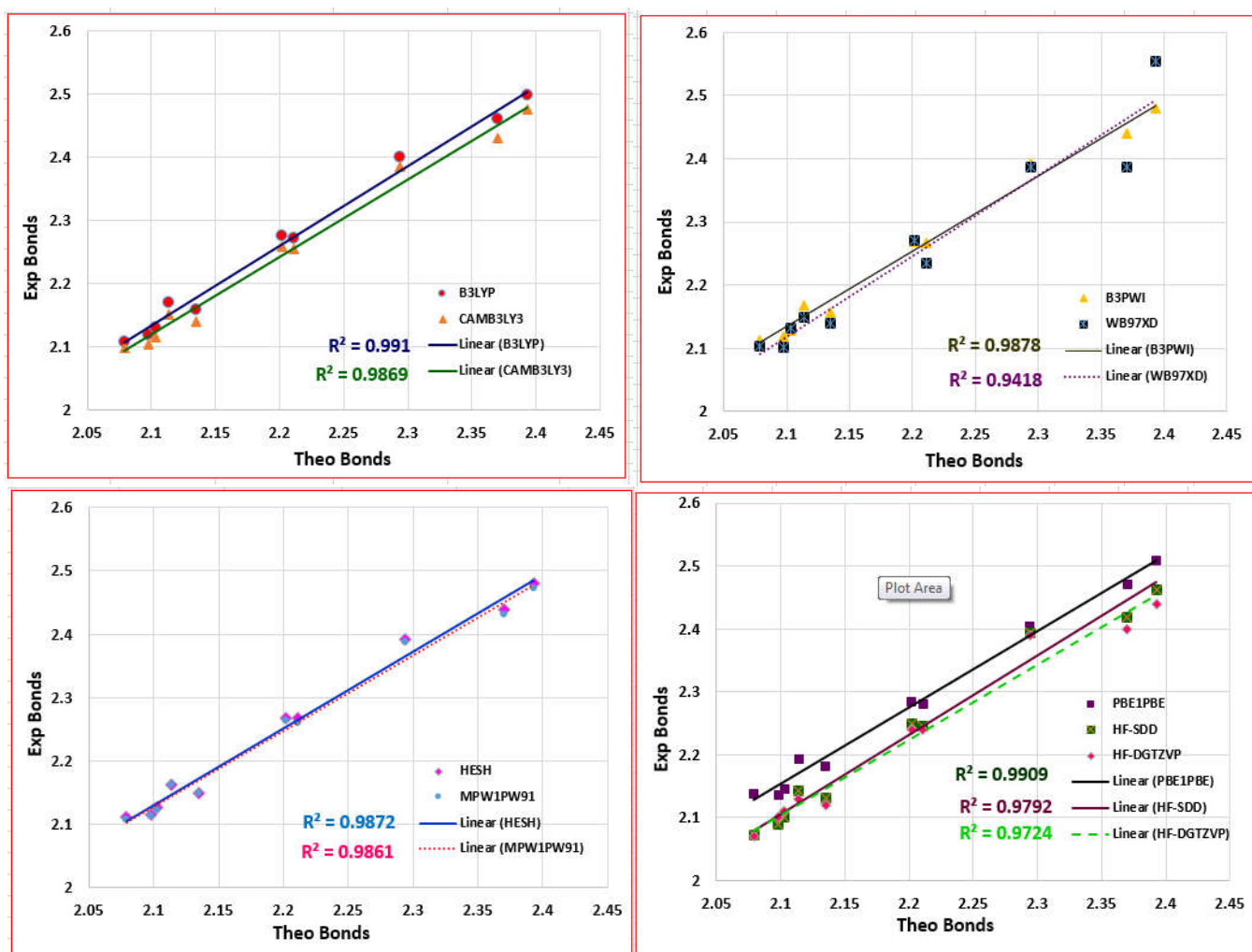


Figure 2. The correlation between the experimental and theoretical bond length (\AA) and angle ($^\circ$)

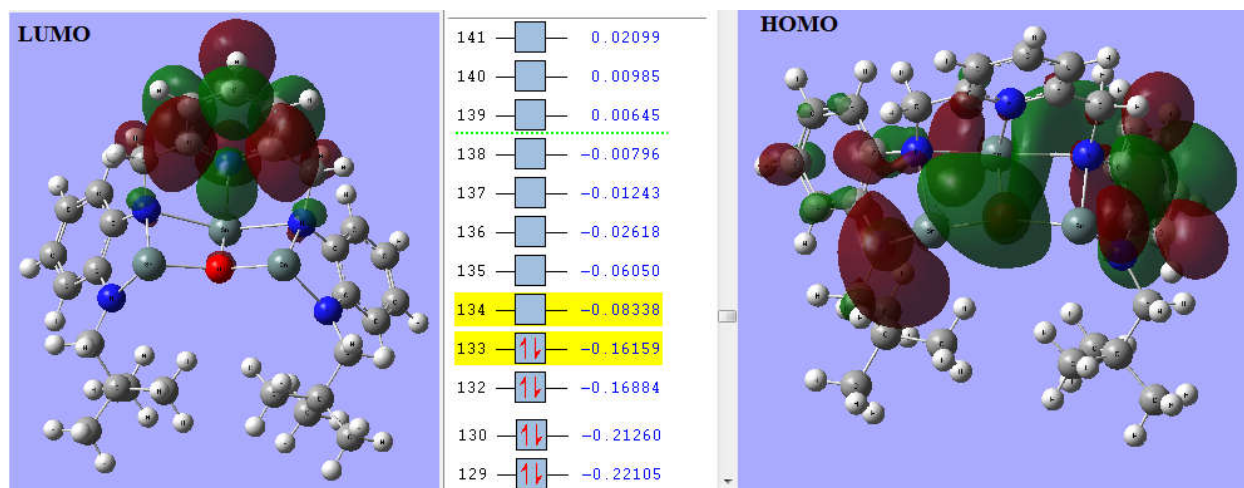


Figure 3. HOMO/LUMODiagrams of the geometry optimized (B3LYP/SDD) indicating significant LUMO electron density is on the lutidinemoiety

Such low energy gap candidates this molecule to be a good semiconductor and solar material. The reason behind this small gap is the existence of the metallic element Sn due to their availability in the HOMO energy level. The calculated Mulliken atomic charges: Sn_1 : 0.878265, Sn_2 : 0.878265, Sn_3 : 1.013248, O_4 : -1.000728, N_5 : -0.587542, N_6 : -0.708129,

N_7 : -0.306266, N_8 : -0.699139, N_9 : -0.577389. The calculated dipole moment and quadrupole moment are 7.5295 Debye and 10.1702 Debye-Ang respectively. The NMR spectrum Figure 4 shows that Sn_3 is more shielded than Sn_2 and Sn_1 due to π - π transition of the electrons from the oxygen and nitrogen atoms to Sn_3 p-orbitals.

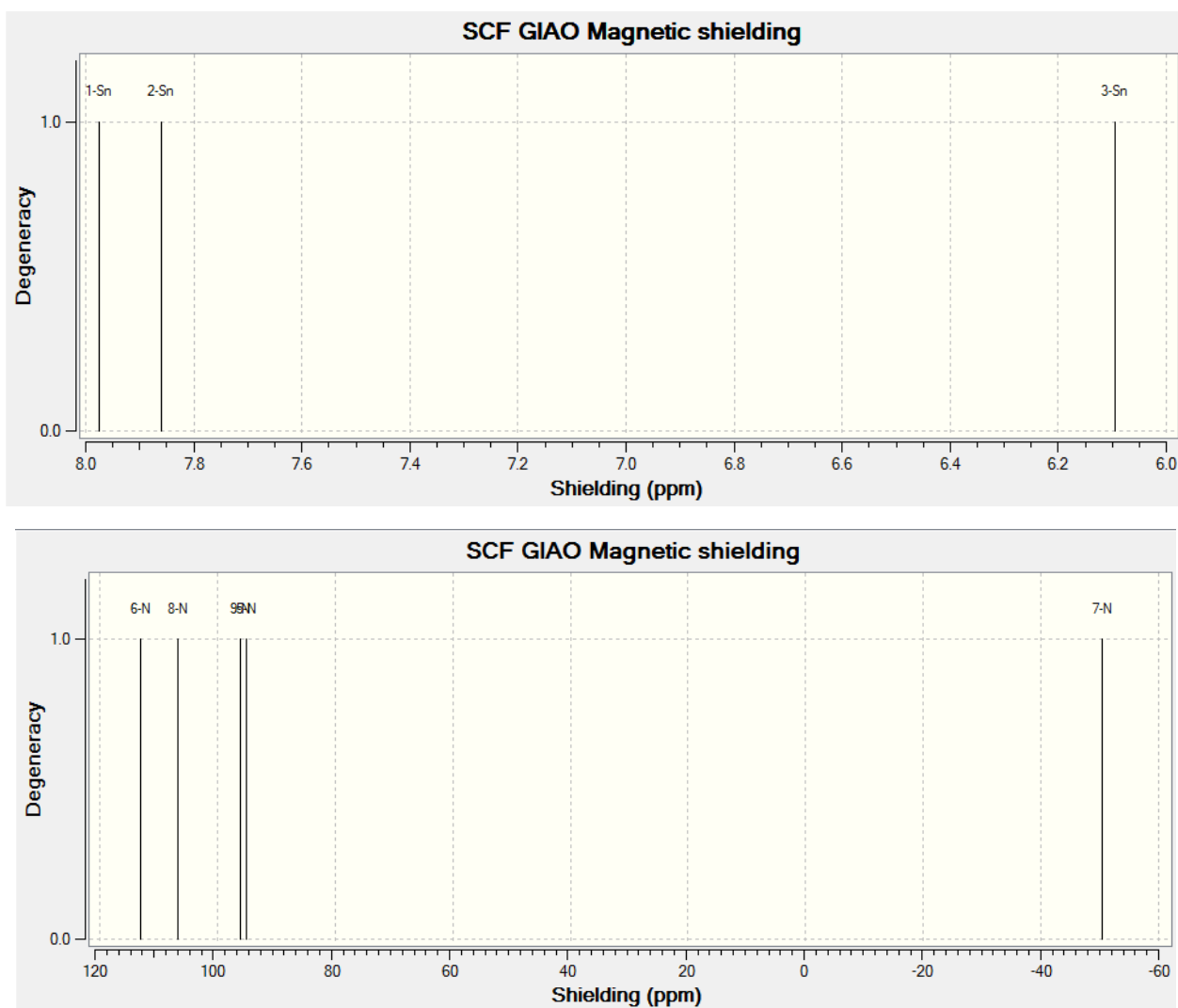
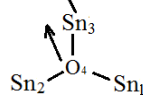
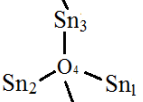


Figure 4. The calculated Sn- and N-NMR of BLBTM molecule

Table-2 Theoretical IR bands of BLBTM molecule

No	Absorption band	mode	atoms
1	σ :139.35 (17)	rocking	ϕ -N ₈ -Sn ₃ -N ₆ - ϕ
2	ν_{as} :175.86 (3.4), 465.22 (32), 492.93 (42)	asy. Stre	Sn ₃ -O ₄
3	ν_s :181.82 (6.8)	systre	Sn ₂ -N ₉
4	δ_{up} :203.14(2.8), 230.64 (2.8), 254.67 (2), 276.77 (7), 286.38 (16.4), 310.82(22.9), 313.77(8.8)	O ₄ out-of-plan up toward N ₇	N ₇ 
6	δ : 225.16 (7.7), 222.95, (8.7), 218.34(8.6)	bending	Sn ₃ -N ₃
7	δ_{down} :286.83(16.4), 230.76(2.8)	O ₄ out-of-plan down from N ₇	N ₇ 
8	ν_{as} :326.74 (26.4) ,387.21 (12.6)	asystre	N ₈ -Sn ₃ -N ₆
9	ν_{as} :358.74 (2.6)	asystre	N ₈ -Sn ₃ -N ₆ + Sn ₃ -O ₄
10	ν_s :439.26 (12.4)	sy. stre	Sn ₂ -O ₄
11	ν_s :548.64(10.7)	systre	Sn ₃ -N ₇ + Sn ₃ -O ₄ + N ₈ -Sn ₃ -N ₆
12	ν_{as} :551.68 (12.5), 770.8, (76.8),	asystre	N ₈ -Sn ₃ -N ₆
13	ν_s :473.98 (148.8)	sy. stre	Sn ₁ -O ₄
14	ν_s :478.42 (11.6)	sy. stre	Sn ₃ -O ₄
15	ν_s :499.55(145.6)	sy. stre	Sn ₁ -O ₄ -Sn ₂
16	δ_{out} :996(74.4)	out-of-plane	N ₈ -Sn ₃ -N ₆

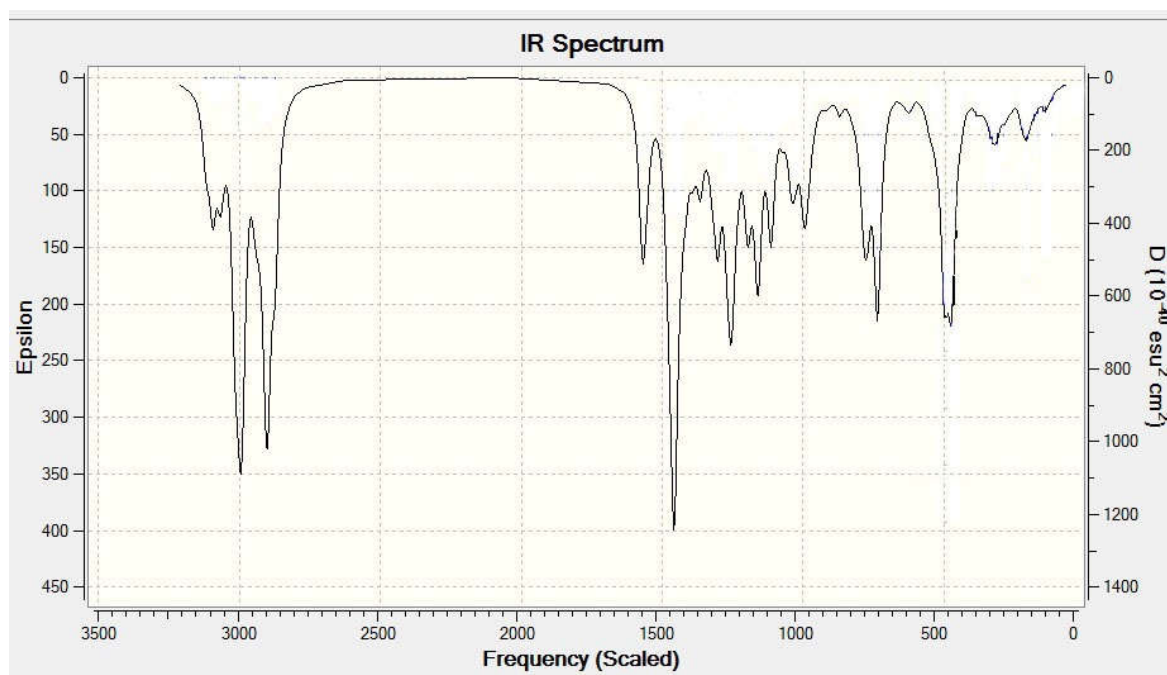


Figure 5. The IR spectrum of the BLBTM molecule calculated at B3LYP/SDD level

The N_7 is more shielded than N_5 , N_6 , N_8 and N_9 and appeared at low field shift with difference of 147 pm.

Theoretical IR Spectrum

We calculated the infrared frequencies for BLBTM using the hybrid B3LYP functional as it was the best among the others focusing on Sn-O and Sn-N bonds. The stretching frequency for the oxygen within the triangle of the three tin atoms; Sn_1 , Sn_2 and Sn_3 appeared at 473.98 (148.8%), 439.26 (12.4%) and 478.42 (11.6%) cm^{-1} respectively. The lowest intensity of Sn_3-O_4 bond possibly due the extra electron density gained from N_8 and N_6 which made it very tight. In addition to the high electron density on Sn_3 atom, it is coordinated by four bonds while Sn_2 and Sn_1 are triply coordinated. The two nitrogen atoms linked to Sn_3 atom showed a strong out-of-plane vibrational band at 996 (74.4%) cm^{-1} . The oxygen atom O_4 is oscillating between Sn_1 and Sn_2 showing very strong frequency at 499.55(145.6) cm^{-1} . The Sn_3-O_4 bond also shows several vibrational bands due to the up and down out-of-plane motion. The IR absorption bands are shown in Figure 5.

Conclusions

The optimized structure of benzannulatedlutidine bisstannylene-tin(II) monoxide molecule BLBTM has been studied by DFT with different functionals where B3LYP with SDD basis set give the best geometrical parameters which is very close to X-ray structures. DFT calculations gives a detailed structural and energetic comparison between experimental and theoretical geometries. The calculated HOMO/LUMO energy gap is of very low energy equals to 85.46meV due to Sn atoms spatial configuration. This low energy gap indicate that this molecule is very suitable to be a semiconductor material. The N_7 and Sn_3 appeared at low field shift in comparison of their peers.

REFERENCES

- Alessandro, B. C. S.; Angelo, A. T. da S.; Tarcizio, J. dos S. F.; Pedro T. W. B., *J. Tetrahedron Letters*, 2009, 50, 2744–2746.
- Alexander V. Z.; Tania P.; Alexander H.; Falko M. S.; Ute C. R.; Rainer P.; Ekkehardt F. H., *J. Am. Chem. Soc.* 2008, 130, 5648–5649.
- Arp, H.; Baumgartner, J.; Marschner, C.; Müller, T., *J. Am. Chem. Soc.*, 2011, 133(15), 5632–5635.
- Bernard, J., *Microchimica Acta*, 1992, 109, (1-4), 5-12
- Braunschweig, H.; Dewhurst, R. D.; Hammond, K.; Mies, J.; Radacki, K.; Vargas, A. *Science* 2012, 336, 1420.; Jones, C.; Sidiropoulos, A.; Holzmann, N.; Frenking, G.; Stasch, A. *Chem. Commun.* 2012, 48, 9855.; Wang, Y.; Xie, Y.; Wei, P.; King, R. B.; Schaefer, H. F., III; Schleyer, P. V. R.; Robinson, G. H. *Science* 2008, 321, 1069.
- De Proft, F. *et al, Organometallics*, 2013, 32 (7), 2121–2134.
- Erickson, J.D.; Fettingner, J.C.; Power, P.P., *Inorg. Chem.* 2015, 54 (4), 1940–1948; Arp, H.; Baumgartner, J.; Marschner, C.; Zark, P.; Müller, T., *J. Am. Chem. Soc.*, 2012, 134, 10864–10875; Hahn, F. E.; Heitmann, D.; Pape, T. *Eur. J. Inorg. Chem.* 2008, 1039–1041.
- Hahn, F. E., *Angew. Chem., Int. Ed.* 2006, 45, 1348–1352; Marion, N.; Díez-González, S.; Nolan, S. P. *Angew. Chem., Int. Ed.* 2007, 46, 2988–3000; Enders, D.; Niemeier, O.; Henseler, A. *Chem. Rev.* 2007, 107, 5606–5655; Trnka, T. M.; Grubbs, R. H., *Acc. Chem. Res.* 2001, 34, 18–29.
- Hashimoto, H.; Odagiri, Y.; Yamada, Y.; Takagi, N.; Sakaki, S.; Tobita, H.; *J. Am. Chem. Soc.*, 2015, 137 (1), 158–161; Sen, S. S.; Khan, S.; Samuel, P. P.; Roesky, H.W.; *Chem. Sci.*, 2012, 3, 659; Hill, N. J.; West, R., *J. Organomet. Chem.* 2004, 689, 4165–4183.
- Hopkinson, M. N.; Richter, C.; Schedler, M.; Glorius, F., *Nature*. 2014, 510, 485–496; Herrmann, W.A.; Köcher, C.,

- Angew. Chem.* 1997, 109, 2256; *Angew. Chem. Int. Ed. Engl.* 1997, 36, 2162; Weskamp, T.; Böhm, V. P.W.; Herrmann, W. A., *J. Organomet. Chem.* 2000, 600, 12.
- Martin, D.; Melaimi, M.; Soleilhavoup, M.; Bertrand, G. *Organometallics* 2011, 30, 5304; Crabtree, R. H. *Coord. Chem. Rev.* 2013, 257, 755.
- Navakoski, de Oliveira K.; Andermark, V.; Onambele, L. A.; Dahl, G.; Prokop, A.; Ott, I., *Chem. Med. Chem.* 2013, 8(02).
- Neumann, W. P. *Chem. Rev.*, 1991, 91 (3), 311–334; Hlina, J.; Baumgartner, J.; Marschner, C.; Albers, L.; Müller, T., *Organometallics*, 2013, 32, 3404–3410; Walewska, M.; Baumgartner, J.; Marschner, C., *Chem. Commun.* 2015, 51, 276.
- Ochiai, T.; Franz, D.; Irran, E.; Inoue, S., *Chemistry - A European Journal*, 2015, 21, (18), 6704–6707; Hahn, F.E. et al., *J. Am. Chem. Soc.* 2008, 130, 5648–5649.
- Sindlinger C. P.; Wesemann, L., *Chem. Commun.*, 2015, DOI: 10.1039/c5cc03425f;
